



PACIFIC EARTHQUAKE ENGINEERING RESEARCH CENTER

Investigation of Sensitivity of Building Loss Estimates to Major Uncertain Variables for the Van Nuys Testbed

Keith A. Porter

James L. Beck

Rustem V. Shaikhutdinov

California Institute of Technology

Investigation of Sensitivity of Building Loss Estimates to Major Uncertain Variables for the Van Nuys Testbed

Keith A. Porter

James L. Beck

Rustem V. Shaikhutdinov

California Institute of Technology

PEER Report 2002/03
Pacific Earthquake Engineering Research Center
College of Engineering
University of California, Berkeley

August 2002

Abstract

A major component of a building-specific seismic loss analysis is the estimation of repair costs in future earthquakes. A number of uncertain variables contribute to the uncertainty in these cost estimates. Among these are ground-shaking intensity, details of the ground motion, mass, damping, and force-deformation behavior, component fragility, repair methods, contractor's direct costs, and contractor's overhead and profit, among others. This report addresses which of these significantly contribute to the overall uncertainty in future economic performance. We examine gross sensitivity by measuring the variation (or swing) of the economic performance when each variable is taken at its assumed median value and at its extremes, e.g., the 10th and 90th percentiles.

Such a study is undertaken for a 1960s nonductile reinforced-concrete moment-frame building located in Van Nuys, California, which is one of two buildings studied by the PEER testbeds program. Here, economic performance is measured in terms of the repair costs associated with the (uncertain) highest shaking intensity the site will experience in the next 50 years. Repair costs are estimated using the assembly-based vulnerability (ABV) method and the site's seismic hazard.

We do not address all uncertainties. Notable among those excluded are the selection among competing models of hysteretic behavior of structural elements, the potential that fragility tests of structural and nonstructural elements do not accurately reflect actual field conditions, the selection among competing repair methods given a component damage state, the choice of nonunion versus union labor to perform repairs, and the potential for repair costs after an earthquake to be increased by demand-driven inflation (a phenomenon often called *demand surge*). Except for demand surge, all of these uncertainties can be examined in future ABV analyses.

The study shows that among the parameters considered here, the top three contributors to uncertainty in earthquake repair cost, in decreasing order, are assembly capacity (i.e., for a building element, the relationship between physical damage and the relevant engineering demand parameter), shaking intensity (measured here in terms of damped elastic spectral acceleration, S_a), and details of the ground motion conditioned on S_a . Uncertainties in parameters of the

structural model contribute modestly to overall uncertainty in economic performance, and are comparable in importance to the uncertainty in the unit costs that a contractor will experience in repairing the damage.

These observations are based only on the demonstration building, but they do offer intriguing implications for performance-based earthquake engineering. If duplicated for other buildings, it may be that much performance uncertainty could be reduced through more-detailed study and modeling of building component damageability. In addition, seismic loss analyses might reasonably neglect uncertainties in structural modeling parameters, without substantially underestimating overall uncertainty.

Acknowledgments

This work was supported in part by the Pacific Earthquake Engineering Research Center through the Earthquake Engineering Research Centers Program of the National Science Foundation under Award number EEC-9701568.

Additional support was provided by the Consortium of Universities for Research in Earthquake Engineering, through the CUREE-Kajima Phase IV Joint Research Program.

Ray Young and John Machin of Ray Young & Associates provided the unit-cost estimates as well as valuable advice regarding cost-estimation practice. Alice Rissman of Rissman and Rissman Associates provided copyrights to the architectural and structural drawings. Carlos Rocha of Rocha Nueze & Associates met with the authors to discuss his seismic retrofit design for the demonstration building. The authors thank these individuals for their contribution.

Contents

Abstract.....	iii
Acknowledgments.....	v
Table of Contents.....	vii
List of Figures.....	ix
List of Tables.....	xi
1. Introduction.....	1
1.1 Motivation.....	1
1.2 Objectives.....	2
2. Analytical Approach.....	5
2.1 Overview of PEER Performance-Based Earthquake Engineering Methodology.....	5
2.2 Assembly-Based Vulnerability.....	7
3. Uncertainty in Basic Input Variables.....	11
3.1 Characterizing Uncertainty in Shaking Intensity.....	11
3.2 Selecting Recordings for Use in the Sensitivity Study.....	12
3.3 Uncertainty in Mass.....	13
3.4 Uncertainty in Viscous Damping.....	14
3.5 Uncertainty in Force-Deformation Relationships.....	16
3.6 Uncertainty in Assembly Capacity.....	18
3.7 Uncertainty in Contractor Costs.....	19
4. Case Study: Van Nuys Hotel.....	21
4.1 Building Description.....	21
4.2 Site Hazard and Ground-Motion Selection.....	24
4.3 Structural Model.....	27
4.4 Assembly Capacity and Repair Costs.....	28
5. Study Results.....	33
6. Conclusions.....	37
References.....	39

List of Figures

Fig. 1. PEER performance-based earthquake engineering methodology overview.	6
Fig. 2. Equivalent viscous damping ratios (McVerry, 1979, left; Camelo <i>et al.</i> , 2001, right). ...	14
Fig. 3. Location of the demonstration building is at “+” symbol near “405” freeway symbol. ..	22
Fig. 4. Column plan.	23
Fig. 5. South frame elevation (omitting stair tower at west end).	23
Fig. 6. Site hazard.	25
Fig. 7. Results of the sensitivity study.	34

List of Tables

Table 1. Uncertainty in damping ratio implied by system ID from strong-motion data.	15
Table 2. Uncertainty in damping ratio associated with analytical approach.	16
Table 3. Recordings considered for representing lower-bound, median, and upper-bound ground-motion time histories.	26
Table 4. Summary of assembly fragility parameters.	30
Table 5. Summary of unit repair costs.	31
Table 6. Parameters of the sensitivity study.	33
Table 7. Summary of results.	34

1. Introduction

1.1 Motivation

Uncertainty is generally costly in earthquake engineering. If one wants to ensure a minimum level of performance with a certain probability, then greater uncertainty in either seismic demand or capacity increases the level of nominal capacity that must be designed into the system. If one can reduce uncertainty, one can generally reduce cost. But there are many sources of uncertainty in earthquake engineering performance: shaking intensity, details of future ground motions with that intensity level, a variety of physical characteristics of the structure in question, construction and repair costs, and details of occupancy and use.

One can assess and possibly reduce uncertainties in each one, but which are the important ones deserving the most attention? By important variables, we mean the ones whose uncertainty contributes most strongly to overall uncertainty in seismic performance. There are two benefits to knowing the relative contribution of each variable to overall uncertainty in a performance metric. First, the variables that do not contribute much to overall uncertainty can be reasonably be taken at their best-estimate value, rather than treated as uncertain, thereby simplifying the analysis problem. Second, the variables that do contribute strongly to overall performance uncertainty can then be the focus of study to understand them better and perhaps reduce their uncertainty.

This report presents a study of future earthquake economic performance. It categorizes the variables that might contribute to overall performance uncertainty, and presents a simple methodology for evaluating their relative contribution. The methodology is illustrated using an engineered commercial building that has been the focus of a broader study by the authors on seismic vulnerability and real-estate investment decision-making [Beck *et al.*, 2002].

1.2 Objectives

To determine the important uncertain variables of earthquake performance, we perform a deterministic sensitivity study that is sometimes employed in decision analysis. In decision analysis, a figure called a *tornado diagram* is commonly used to illustrate the sensitivity of an uncertain future value to the more-basic input variables that contribute to it. The output must be a known deterministic function of a variety of input variables, and either the value or the probability distribution of each of the input variables must be specified.

The output variable, as a deterministic function of one or more uncertain inputs, is studied using a series of deterministic tests. In the first test, each input variable is set to its best-estimate value, and the output is measured. Then one input is set to an extreme value (a low or high value), and the output measured again. The input is then set to the other extreme, and the output is measured. The absolute value of the difference between the outputs from these two cases is a measure of the sensitivity of the output to that input variable. This difference is called the *swing*. The first input is then set to its best-estimate value, and the process repeated for the next input, to determine the swing associated with the variability of that input. One then ranks the input variables according to their swing. A larger swing reflects a more-important input uncertainty.

Our objective is to perform such a study for a demonstration building, with the output parameter of interest being the total repair cost, and the input variables being those that significantly affect the repair cost, with the exception of parameters that are unrelated to the pre-earthquake building condition, the site, or the seismic conditions.

The demonstration building should be real, preferably one studied under PEER's testbeds program, to facilitate comparison with other studies and to employ to the extent possible PEER's performance-based earthquake engineering (PBEE) methodology. The building should be representative of a common class of structures, both in its construction and use. The study should not rely on expert opinion.

The basic uncertain variables to be considered include all those that significantly affect the future repair cost given the occurrence of a future earthquake, namely,

1. Ground motion intensity
2. Details of ground motion

3. Building mass
4. Viscous damping
5. Parameters of the force-deformation relationship for the structural elements
6. Capacity of building assemblies to resist damage
7. Contractor unit costs
8. Contractor overhead and profit

Other parameters could significantly affect the future repair costs, such as ground failure (e.g., liquefaction), the repair method employed to repair a given type of damage, and the choice of union versus nonunion labor to perform repairs. As potentially important as these are, we ignore them here. We also ignore building-code changes that might require the repair efforts to restore the building to greater than its pre-earthquake condition; post-earthquake cost inflation (so-called *demand surge*); errors induced by idealization of force-deformation behavior; and post-earthquake tenant improvements and other architectural program changes by the owner.

2. Analytical Approach

2.1 Overview of PEER Methodology

The analytical approach employed in the present study is intended to be consistent with PEER's performance-based earthquake engineering (PBEE) methodology, so an overview of that developing methodology is appropriate here. PEER's PBEE objective is to quantify overall facility performance as a function of location and design. Performance will be measured in terms of one or more decision variables (DVs) that are of direct interest to the facility stakeholders, such as future earthquake repair cost, downtime, or life safety. The value of the methodology is in its ability to inform the stakeholders' decision of selecting between competing facility design alternatives: where to build, what structural and nonstructural systems to use, and what strength and stiffness to provide to those systems.

As of this writing, the PEER methodology is still in development, but as currently envisioned, it has four distinct sequential analytical elements: hazard analysis, structural analysis, damage analysis, and what is referred to here as loss analysis. The methodology is summarized in Fig. 1, and embodied schematically in the following framing equation, which is based on the theorem of total probability:

$$g[DV] = \int_{DM} \int_{EDP} \int_{IM} p[DV | DM] p[DM | EDP] p[EDP | IM] g[IM] dIM dEDP dDM \quad (1)$$

where

DV = decision variable: the performance parameter of direct interest such as repair cost

DM = damage measure: a scalar or vector parameter measuring physical damage

EDP = engineering demand parameter: a scalar or vector measure of structural response

IM = intensity measure: a scalar or vector parameter measuring earthquake site effects

$p[\cdot]$ = probability density of the quantity inside the brackets

$g[IM]$ = mean rate of occurrence of events with intensity IM (rate per unit of IM)

$g[DV]$ = mean rate of occurrence of events with value DV of the decision variable

Each density function represents one element of the analysis methodology: $g[IM]$ reflects the results of the hazard analysis; $p[EDP|IM]$ reflects the structural analysis; $p[DM|EDP]$ represents the damage analysis; and $p[DV|DM]$ reflects the loss analysis. The detailed definition of each of the parameters remains to be developed, and may vary by facility type, location, and decision-maker.

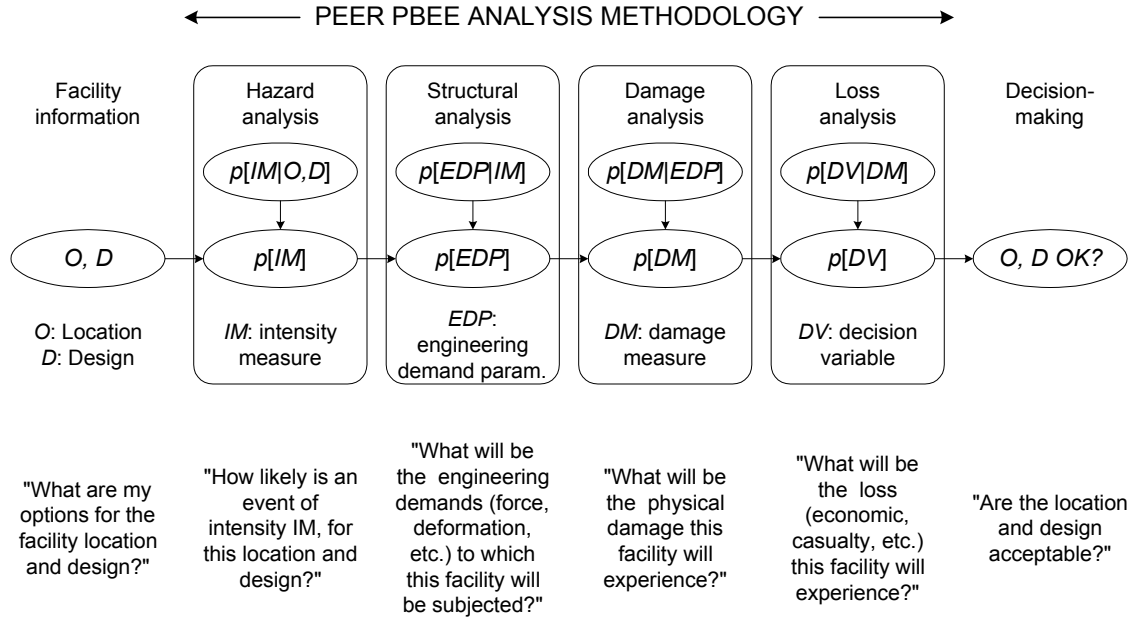


Fig. 1. PEER performance-based earthquake engineering methodology overview.

The figure highlights some important features of the PEER methodology:

1. The DV is explicitly quantified as a function of facility location and design.
2. The steps in the analysis are compartmentalized by professional specialty: the hazard analysis can be performed by seismologists and geotechnical engineers with limited knowledge of structural engineering issues. Similarly, the structural analysis can be performed by structural engineers without specialized knowledge of the steps that come before or after.
3. The methodology is probabilistic: in each analysis, the input and the output are either explicit probability distributions, or otherwise account for the uncertainties involved.

One likely form of the methodology extends reliability principles employed in load and resistance factor design from an inequality on component strength demand and capacity to an inequality on overall structural drift. That is, one would apply factors to calculated drift response and to drift capacity, and ensure that the factored response does not exceed the factored capacity. This approach requires that structural response can be used as a proxy for decision variables such as repair cost, loss of use, and casualties. This in turn requires that sufficiently general relationships can be created between response and the decision variables of interest, as hypothesized in FEMA 273 and FEMA 356 (Federal Emergency Management Agency, 1997, 2000). This vision of the PBEE methodology makes the probabilistic aspects mostly implicit, hidden from the engineering practitioner. Furthermore, it largely eliminates the last two steps, damage and loss analysis, for which current practitioners are largely unprepared.

Current challenges to the completion of PEER's methodology include the choice of parameterization of the variables IM , EDP , DM , and DV , the formulation of the conditional distributions $p[EDP|IM]$, etc., and the numerical technique for evaluating the quadruple integral. The details of the methodology must address the quantification and propagation of uncertainty in each step, and the treatment of correlation within vector variables (e.g., between different elements of EDP such as between story drifts). If an EDP is used as a proxy for performance (i.e., if the damage and loss analysis are truncated from the methodology, as in the case of FEMA 273 [Federal Emergency Management Agency, 1997]), the methodology must deal with potential blindness to design alternatives that affect damage and loss, but not hazard and structural analysis.

The analytical approach employed in the present study is consistent with the PEER framework, and meets many of the desiderata suggested above. With this overview of PEER's PBEE methodology in mind, we now introduce the methodology used here to perform the sensitivity study, namely, the assembly-based vulnerability (ABV) method.

2.2 Assembly-Based Vulnerability

ABV is a framework for estimating earthquake-related repair costs for a building as a function of ground motion intensity. It involves the last three stages in Fig. 1: structural, damage and loss analyses. For an overview of ABV, see Porter *et al.* [2001a].

Briefly, ABV works as follows. The building is conceptualized as a collection of standard assemblies, such as reinforced-concrete beam-columns, wallboard partitions, windows, etc. A value of the ground motion intensity is specified and then a series of simulations is performed involving the following steps. First, one selects a structural model by randomly sampling the structural parameters that are considered uncertain, and then one randomly selects or generates a suite of ground-motion time histories scaled to the desired intensity. A nonlinear time-history structural analysis of the structure is performed for each ground-motion time history in turn. Each structural analysis produces a set of structural responses (member deformations, interstory drifts, floor accelerations, etc.) that are then input to fragility functions for each assembly in the building to randomly sample its damage state. Given the damage state for each assembly, one then randomly samples the direct cost to repair each of these damages and the contractor overhead and profit, and produces a sample of total repair cost. Thus, for each simulation performed, the result is an (S, C_T) sample pair, where S is the shaking intensity of interest and C_T is the total repair cost. Repair cost is usually expressed as a fraction of building replacement cost (denoted by RCN for replacement cost, new). This ratio is referred to as the damage factor, denoted here by $DF = C_T/RCN$.

Each parameter in the process is represented by a random variable: random mass or damping, random damage state conditioned on structural response, etc. Repeated simulations produce a set of (S, DF) pairs of loss estimates that are consistent with the probability distributions on each of the basic random variables (parameters of the structural response, component fragility, contractor costs, etc.).

A wide variety of structures can be studied in this way; to date, the authors have examined hypothetical and real buildings whose structural systems include steel moment-resisting frames, reinforced-concrete moment frames, and wood frames. For a detailed discussion, see Beck *et al.* [1999], Porter and Kiremidjian [2001b], Porter *et al.* [2001c] or Beck *et al.* [2002]. These and other studies have focused on developing probabilistic relationships between loss and shaking intensity for a variety of structures, but have not yet examined the contribution of each basic uncertain variable to the overall uncertainty in loss to the degree addressed here.

ABV is related to PEER's PBEE methodology in that it includes structural, damage and loss analyses stages. The DV is explicitly quantified as a function of facility location and detailed design. It is fully probabilistic, in that in each step of the analysis, the input and the output are expressed as samples of random variables. It employs explicitly defined variables reflecting IM , EDP , DM , and DV . The random sampling addresses the quantification and propagation of uncertainty in each step, and since no information is lost between simulation steps, correlation within vector variables is retained. Since the DV is explicitly evaluated, i.e., no parameter such as drift is used as a proxy for DV , the approach avoids blindness to design alternatives that affect damage and loss, but not hazard and structural analysis.

ABV does not meet one of the desiderata mentioned above: it requires the analyst to perform the damage and loss analysis, which involve skills that are unfamiliar to most structural engineering practitioners, which may hinder ABV from wide acceptance. However, as a research tool, ABV is well suited to address the objectives of this study. Furthermore, current research by the authors suggests that the ABV analysis can be approximated by a simplified procedure that resembles PML calculations that are often done by structural engineers.

With this overview of the analytical approach in mind, we turn now to quantification of the basic uncertain variables for a general structure.

3. Uncertainty in Basic Input Variables

3.1 Characterizing Uncertainty in Shaking Intensity

A variety of ground-motion intensity measures are available. Historically, Modified Mercalli Intensity has been used as a predictor of loss, e.g., ATC-13 [1985], as well as instrumental measures such as peak ground acceleration or the spectral response measures: S_a , S_v , or S_d . Other measures intended to predict building performance have been proposed, e.g., by Cordova *et al.* [2001] and Luco and Cornell [in press]. Two criteria for selection of an intensity measure (*IM*) suggest themselves. First, the *IM* must strongly correlate with the performance variable of interest, such as damage factor (*DF*, the ratio of repair cost to replacement cost). Second, an *IM* is primarily useful insofar as hazard information is available (i.e., information on the occurrence probability of an earthquake with a given *IM* level). Of course, the greater the correlation of an *IM* with the performance variable, the stronger the incentive to develop the hazard information.

The arguments for various *IMs* are familiar: S_a is proportional to the maximum seismic force in a linear elastic SDOF system subjected to an earthquake, and therefore should be related to maximum forces in a similar structure. Similarly, S_d is proportional to the maximum deformation of a linear elastic SDOF system, and therefore should be related to the damage experienced by displacement-sensitive components. The spectral response parameters are essentially interchangeable for light damping, as they are related through $S_a \approx \omega S_v \approx \omega^2 S_d$, where ω is the angular frequency. On the other hand, inelastic response spectral parameters offer the advantages of better reflecting demand on structures that exceed elastic response, through the added parameter of ductility demand.

Luco and Cornell [2001] argue that an *IM* that is selected should be both an efficient and sufficient predictor of damage; efficient in that it is highly correlated with damage, and sufficient in that, conditioned on the *IM*, damage is not significantly correlated with other parameters of ground motion, particularly magnitude and distance.

In the end, the case for one *IM* over another will be made not solely on theoretical considerations, but also on the basis of accumulated evidence of how well it predicts damage for various structures. Since for present purposes we are interested in the variability of repair cost attributable to variability in shaking intensity, it is necessary to use an intensity measure for which occurrence probability is available. Currently, probabilistic seismic hazard information is most readily available for damped elastic spectral acceleration response, S_a , which we therefore use for convenience. (More precisely, we use the S_a for 5% viscous damping at the small-amplitude fundamental period of the building.)

If one assumes Poisson arrivals of earthquakes, the frequency form of the spectral-acceleration hazard function ($G(S_a)$, the annual frequency of events exceeding seismic shaking intensity S_a) can be used to determine the S_a corresponding to a given non-exceedance probability P_0 during a period t , as follows. The number of earthquakes Y whose shaking exceeds S_a in period t is distributed according to the Poisson distribution:

$$P[Y = y] = (\nu t)^y e^{-\nu t} / y! \quad (2)$$

where $\nu = G(S_a)$ is the frequency of occurrences per unit time of events exceeding S_a . Thus, the probability that no earthquakes will occur ($Y = 0$) with shaking exceeding S_a in time t is given by

$$P[Y = 0] = P_0 = e^{-\nu t} \quad (3)$$

One can solve for ν for a given non-exceedance probability P_0 and time t , and hence find the S_a associated with this mean exceedance rate by inverting the hazard function G :

$$S_a = G^{-1}(\nu) = G^{-1}(-\ln(P_0)/t) \quad (4)$$

In this study, we use $P_0 = 0.10$, 0.50 , and 0.90 for $t = 50$ years, i.e., the 10th, 50th, and 90th percentiles for S_a .

3.2 Selecting Recordings for Use in the Sensitivity Study

Ground-motion characteristics other than the primary intensity measure S_a undoubtedly affect the repair costs, but the question remains of how to parameterize these characteristics. A digital ground motion recording can have tens of thousands of data points, rather than one parameter. Two choices present themselves. First, one can perform a large number of loss analyses for a building of interest, each time using a different ground motion scaled to the

intensity of interest. The lower-bound event can be selected as the one that produces the loss closest to some predetermined lower fractile such as the 10th percentile. Likewise, the best-estimate and upper-bound events would be those producing the median and perhaps 90th percentile loss. This approach is simple and provides some information about the degree of effect of detailed ground motion on loss, but offers no insight into why ground motions with equal intensity produce different performance.

A second alternative is to select a secondary intensity measure that is not highly correlated with the primary measure, but that might hypothetically strongly affect loss. From a large sample set of ground-motion recordings scaled to the desired primary intensity measure, one can select lower-bound, best-estimate, and upper-bound ground motions based on this secondary measure. Intensity measures worthy of examination include one recently proposed by Cordova *et al.* [2001]; Arias intensity; and others. In order to pursue this approach, it would be necessary to determine the 2-parameter hazard relationship. For example, one might know both $G(S_a)$ and have a probability distribution on the secondary intensity measure, conditioned on S_a . We hope to pursue this approach in later study, but for the limited purpose of demonstrating the swing associated with detailed ground motion, it is unnecessary. We therefore opt for the first, simpler approach.

3.3 Uncertainty in Mass

Building mass is an uncertain variable for several reasons: as-built member dimensions vary from those shown on the design documents; unit weights are imperfectly known; and actual building components can vary from those assumed in the design, e.g., layers of roofing are often added during the life of the building, which can significantly affect dead load. Ellingwood *et al.* [1980] summarize the conclusions of several authors, who feel that an adequate model for the probability distribution on dead load is the Gaussian distribution, with a mean value equal to the nominal (calculated) dead load, and a typical coefficient of variation of 0.10. Thus, using the 10th and 90th percentiles of the Gaussian distribution as the lower- and upper-bounds of mass, one can take dead load as varying between $0.872D_n$ and $1.128D_n$, where D_n refers to nominal dead load, and the factors 0.872 and 1.128 refer to the inverse of a Gaussian cumulative distribution with unit mean and coefficient of variation of 0.10, evaluated at 0.10 and 0.90, respectively.

3.4 Uncertainty in Viscous Damping

Some experimental data on the variability in viscous damping are available. McVerry [1979] presents results of system identification for 10 instrumented buildings that experienced strong motion in the 1971 San Fernando earthquake. These include five steel-frame buildings, four with reinforced-concrete frames, and one with reinforced-concrete shearwalls. Two of these buildings experienced multiple earthquakes. McVerry [1979] finds that first-mode equivalent viscous damping ratios vary in single buildings between directional components and between earthquakes. Fig. 2 shows his data plotted against peak ground acceleration. The figure shows that the damping ratio appears to be modestly sensitive to shaking intensity, implying that hysteretic damping contributes to the calculated equivalent viscous damping. Camelo *et al.* [2001] present similar results for several instrumented woodframe buildings subjected to strong motion or forced vibration; their data are shown in the right-hand plot of Fig. 2. Note that McVerry [1979] parameterizes intensity via PGA, whereas Camelo *et al.* [2001] use S_a . Within a structure type, damping ratio appears to be modestly sensitive to shaking intensity. Analysis of the data suggests a coefficient of variation for damping ratio of approximately 0.3.

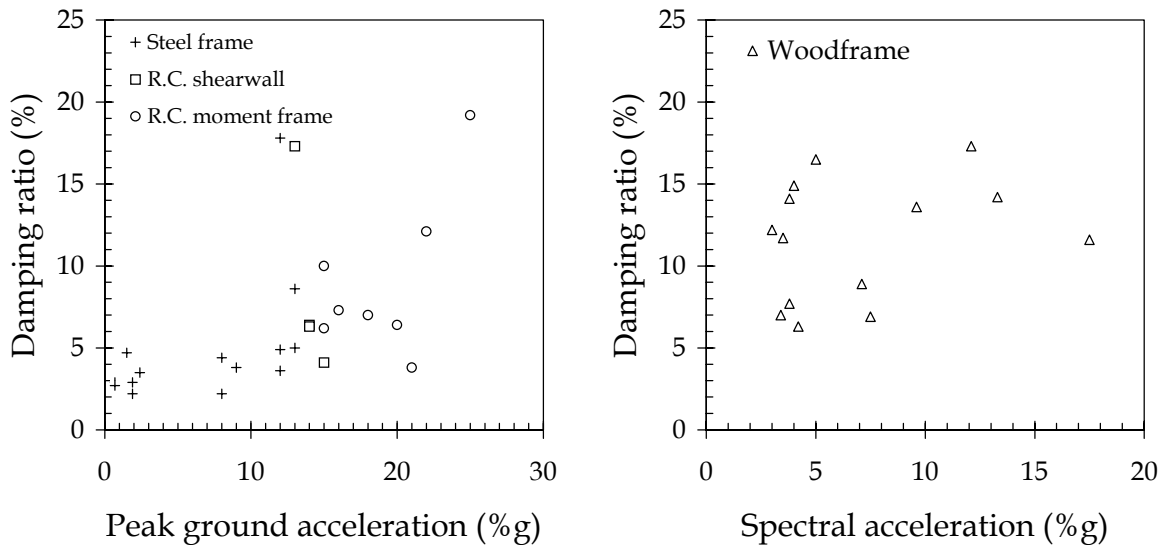


Fig. 2. Equivalent viscous damping ratios (McVerry, 1979, left; Camelo *et al.*, 2001, right).

One can estimate uncertainty in “pure” viscous damping (i.e., aside from damping caused by hysteretic energy dissipation) by examining the scatter of the imputed viscous damping about a regression line at low levels of shaking intensity. Using the scatter about the regression line

should correct to some degree for the mean effect of hysteretic damping, and restricting the analysis to low intensities should further limit the contribution to overall uncertainty from hysteretic damping. Results of a linear regression of these data ($\text{PGA} \leq 0.10\text{g}$ in McVerry [1979], and $S_a \leq 0.10\text{g}$ in Camelo *et al.* [2001]) are shown in Table 1. In the table, β refers to the damping ratio, δ_β denotes the coefficient of variation for damping ratio, R^2 refers to the square of the correlation coefficient between acceleration A (either PGA or S_a) and β , and $\delta_{\beta|A}$ refers to the coefficient of variation for damping, with the assumed mean effect of hysteretic damping removed via

$$\delta_{\beta|A} = \delta_\beta \sqrt{1 - R^2} \quad (5)$$

An additional data point is provided by Taoko [1981], who presents damping ratios determined from forced-vibration tests for two highrise steel-frame buildings in Japan, observing damping ratios for the first few modes to be in the range of 0.5% to 1.5%. The average of the damping ratios is 1.1%; the coefficient of variation, 0.3.

Table 1. Uncertainty in damping ratio implied by system ID from strong-motion data.

Parameter	McVerry [1979]	Camelo <i>et al.</i> [2001]
σ_β	0.90%	3.6%
$E[\beta]$	3.3%	11%
δ_β	0.28	0.34
R^2	0.04	0.00
$\delta_{\beta A}$	0.27	0.34

As noted above, damping statistics for individual structures are not directly observed, but result from system-identification analysis of structures affected by forced vibration or strong ground motion. Beck [1982] shows how the analytical method used to determine the equivalent viscous damping significantly affects the estimate of the damping ratio, implying additional uncertainty beyond that reflected in the scatter of the calculated damping ratios. He compares the equivalent viscous damping ratios calculated for six buildings by McVerry [1979], with those calculated by Hart and Vasdevan [1975] for the same records. Table 2 presents these statistics. The table shows the equivalent viscous damping ratios calculated for the fundamental period in

the direction shown, expressed as a percentage of critical. It also shows the average of the two research teams' estimated values. If one takes the average as the best-estimate value of the "true" damping ratio, then the scatter about the average reflects the uncertainty in damping associated with analytical method. The table shows that the sample standard deviation of the natural logarithm of the Hart estimate divided by the average value has a value of 0.27. This is approximately equal to the coefficient of variation for β_1 associated with analytical technique. (The value would be the same for the McVerry figures).

Table 2. Uncertainty in damping ratio associated with analytical approach.

Building, address (stories, structural system)	Direction	β_1 (%), Hart	β_1 (%), McVerry	β_1 (%), Avg	ln(Hart/Avg)
1900 Ave of the Stars (27, SF)	N44E	5.2	4.4	4.8	0.08
	S46E	6.5	2.2	3.8	0.54
KB Valley Center 15910 Ventura Blvd (18, SF)	S09W	11.3	8.6	9.9	0.14
	S81E	8.9	6.3	7.5	0.17
Sheraton-Universal 3838 Lankershim (20, RC)	N00W	4.9	7.3	6.0	-0.20
	N90W	4.1	6.2	5.0	-0.21
Bank of California 15250 Ventura Blvd (12, RC)	N11E	10.4	12.9	11.6	-0.11
	N79W	9.0	5.8	7.2	0.22
Holiday Inn 8244 Orion Blvd (7, RC)	N90W	16.4	17.3	16.8	-0.03
	N00W	9.7	19.2	13.6	-0.34
Holiday Inn 1640 S Marengo Ave (7, RC)	S52W	8.8	5.0	6.6	0.28
	M38W	9.0	17.8	12.7	-0.34
$\sigma[\ln(\text{Hart}/\text{Avg})] \cong \delta_{\beta a}$					0.27

In light of these observations, we take the coefficient of variation for the damping ratio as the SRSS of the uncertainties associated with the variability between records ($\delta_{\beta r} = 0.3$) and the analytical approach ($\delta_{\beta a} = 0.27$), for a total uncertainty $\delta_{\beta} = 0.4$.

3.5 Uncertainty in Force-Deformation Relationships

Uncertainty in the hysteretic behavior of structural elements results from a variety of sources: as-built members dimensions vary from construction documents; material properties differ from those assumed in the analysis; true stress-strain behavior at the element-fiber level

differs from engineering idealizations; etc. How should one address these uncertainties as they affect the force-deformation relationships of the structural elements? The force-deformation relationships themselves can be quite complex. Idealizations can involve a dozen or more potentially correlated parameters of which the designer has imperfect knowledge. An initial attempt to capture uncertainty in these parameters can be simple or complex. A simple approach would be to scale every force and deformation value on the force-deformation relationship by a single, random variable (let this approach be called *random strength, constant stiffness*). Slightly more complex would be to scale force values on the force-deformation relationship by one random variable, and deformation values by a second, correlated random variable (*random strength and stiffness*). One could also conceivably treat each parameter in the idealized hysteresis model as a random variable related through a covariance matrix. We reject this last approach here in order to concentrate on the general contribution of force-deformation uncertainty to loss uncertainty and so we further examine the two simpler approaches.

Ellingwood *et al.* [1980] summarize research on variability of member resistance. For example, considering the resistance of reinforced-concrete flexural members, they suggest a coefficient of variation for flexural strength of 0.08. They do not treat uncertainty in stiffness, which is also of interest here. Therefore, we performed a simple study of the moment-curvature relationship for a sample reinforced-concrete beam, $b = 16$ in., $d = 20$ in., 3-#8 top bars, 2-#8 bottom bars. We modeled f'_c , concrete crushing strain ϵ_c , and steel yield stress f_y as Gaussian random variables with $E[f'_c] = 8.3$ ksi, $\delta[f'_c] = 0.18$, $E[\epsilon_c] = 0.0035$, $\delta[\epsilon_c] = 0.05$, $E[f_y] = 67.5$ ksi, and $\delta[f_y] = 0.098$, where $E[\cdot]$ and $\delta[\cdot]$ refer to the expected value and coefficient of variation, respectively, for the variable inside the brackets. We then used UCFyber [ZEvent, 2000] to find yield and ultimate moments and curvatures. After 20 simulations, we found a coefficient of variation for yield strength (M_y) and yield curvature (ϕ_y) of 0.084 and 0.080, respectively, with a high correlation coefficient ($\rho_{M_y, \phi_y} = 0.96$). We found coefficients of variation for ultimate strength (M_u) and curvature at ultimate of 0.008 and 0.093, respectively, with a correlation coefficient $\rho_{M_u, \phi_u} = 0.76$. That this experiment produces an overall coefficient of variation for yield strength similar to that of Ellingwood *et al.* [1980], and high correlation between moment and curvature, argues for the random-strength, constant-stiffness approach. The random-strength, constant-stiffness model overstates by an order of magnitude the coefficient of variation

for ultimate strength. Nonetheless, we find the random-strength, constant-stiffness model reasonably approximates the moment-curvature behavior of reinforced-concrete flexural members.

Another issue is how the hysteretic behavior of different elements is correlated. Perfect correlation would mean, for example, that if element i were 20% stronger than nominal, so is element j . Perfect correlation would tend to produce greater uncertainty in overall structural response, and therefore represents a conservative approach. Zero correlation would mean that knowledge of the strength of element i tells one nothing about element j . In this study, for simplicity and to be conservative regarding uncertainty, we assume perfect correlation.

The random-strength, constant-stiffness model also appears to be reasonable for steel moment-resisting frames. The elastic modulus (E) and dimensions of rolled steel sections (and hence moment of inertia, I) have little uncertainty, and these parameters determine stiffness, whereas steel strength is less certain. Ellingwood *et al.* [1980] suggest coefficients of variation for resistance of steel structural members between 0.1 to 0.3, somewhat greater than the strength uncertainty for reinforced-concrete flexural members.

3.6 Uncertainty in Assembly Capacity

Assembly fragility is defined as the probability of an assembly exceeding some undesirable limit state (e.g., repairable damage to a building component such as a nonstructural partition) conditioned on some demand parameter (e.g., a structural response parameter such as interstory drift ratio). It is often conveniently modeled as a fragility function, which is a cumulative probability distribution whose random variable is the demand parameter. The larger the dispersion in the probability distribution, the greater the uncertainty in the threshold level of demand that leads to the specified damage. One can select lower-bound, best-estimate, and upper-bound values of assembly capacities by selecting a probability level corresponding to each, and inverting the fragility function at that probability level.

Given a probability distribution, it is straightforward to evaluate the 10th, 50th, and 90th percentiles of the demand-parameter distribution as the lower-bound, best-estimate, and upper-bound capacity of the assembly. It is common to use the lognormal distribution to describe the fragility of many assemblies. The P fractile of the lognormal is given by

$$X_P = x_m \exp(\beta \Phi^{-1}(P)) \quad (6)$$

where X_P is the demand parameter associated with probability P that the assembly will be damaged, β is the logarithmic standard deviation of the distribution, $\Phi^{-1}(P)$ is the inverse of the standard Gaussian cumulative distribution evaluated at P , and x_m is the median of the distribution. The probability P is taken as 0.1 for the 10th percentile, 0.5 for the 50th, etc.

A variety of component fragility functions and their parameters are presented in Beck *et al.* [1999], Porter *et al.* [2001c], and Beck *et al.* [2002]. These are developed using laboratory test data for most assemblies, and theoretical considerations (i.e., reliability methods) for the remainder.

3.7 Uncertainty in Contractor Costs

Two types of costs are considered here: unit costs and contractor overhead and profit. By *unit costs* we mean the cost to restore a single unit of a damaged assembly to the undamaged state. Construction cost estimators typically compile construction cost estimates by describing the work to be performed in terms of a standard taxonomic system, often by the Unifomat system [American Society for Testing and Materials, 1996]. The work to be performed is then measured in quantities of each taxonomic group. The cost for each task is calculated as the quantity of work times a cost per unit. The sum of the costs for the tasks is the direct cost; to this must be added indirect costs that are not attributable to tasks, such as administration, permits, mobilization, etc., and the contractor's profit. Together, overhead and profit tend to range between 15% and 20% of the direct cost, with larger jobs tending to have a lower factor for overhead and profit.

Unit-cost estimates carry some degree of uncertainty for various reasons: variability in costs of materials and of labor, uncertainty in the productivity of the workers, etc. With some exceptions, empirical data on the magnitude of this uncertainty are largely lacking. RS Means Corp. [1997], which performs extensive surveys of construction costs in the United States, recommends a cost contingency of 20% for the overall cost of a repair project, suggesting a coefficient of variation for total repair costs of approximately the same order of magnitude, perhaps 15 to 20%. Alternatively, construction cost estimators can determine the uncertainty in particular unit costs based on their experience.

4. Case Study: Van Nuys Hotel

4.1 Building Description

With this overview of the parameters of interest, their sources and magnitudes, we present a demonstration study of the sensitivity of loss to uncertainty in each basic random variable. This is a companion study to a full probabilistic ABV analysis of the same building, presented in Beck *et al.* [2002], which does not include a sensitivity analysis of the uncertainties.

The demonstration building is a 7-story, 66,000 sf (6,200 m²) hotel located at 8244 Orion Ave, Van Nuys, CA, at 34.221° north latitude, 118.471° west longitude, in the San Fernando Valley of Los Angeles County, California. The location is shown in Fig. 3. The building has been studied extensively, e.g., by Jennings [1971], Scholl *et al.* [1982], Islam [1996a, 1996b], Islam *et al.* [1998], Li and Jirsa [1998], and Browning *et al.* [2000]. To date, it appears that no researcher has assessed the seismic vulnerability of the building in terms of repair cost as a function of shaking intensity, or examined the effect of various uncertain variables on overall uncertainty in economic performance.

The hotel was designed by Rissman and Rissman Associates [1965] according to the 1964 Los Angeles City Building Code, and built in 1966. The lateral force-resisting system is a perimeter reinforced-concrete moment frame in both directions. The building was lightly damaged by the M6.6 1971 San Fernando event, approximately 20 km to the northeast, and severely damaged by the M6.7 1994 Northridge earthquake, whose epicenter was approximately 4.5 km to the southwest. After the 1994 earthquake, the building was retrofitted with new reinforced-concrete shearwalls, but we examine the building as it existed just before the earthquake. Floor plans, elevations, and column and beam reinforcement details and schedules can be found in Beck *et al.* [2002].

The column plan (with the designer's column numbers) is shown Fig. 4. In the figure, "C1" through "C36" refer to the designer's column numbering. The plan is regular, with three

bays in the transverse direction, eight in the longitudinal direction. In this analysis, the south frame is analyzed, and the nonstructural components in each story for the south half of the building are modeled using interstory drifts at the south frame. The frame is regular in elevation, as shown in Fig. 5. The figure shows the designer's notation for beam and column numbering. Columns in the south frame are 14 in. wide by 20 in. deep, i.e., oriented to bend in their weak direction when resisting lateral forces in the plane of the frame. Spandrel beams in the south frame are generally 16 in. wide by 30 in. deep at the 2nd floor, 16 in. wide by 22-½ in. deep at the 3rd to 7th floors, and 16 in. wide by 22 in. deep at the roof.



Fig. 3. Location of the demonstration building is at “+” symbol near “405” freeway symbol.

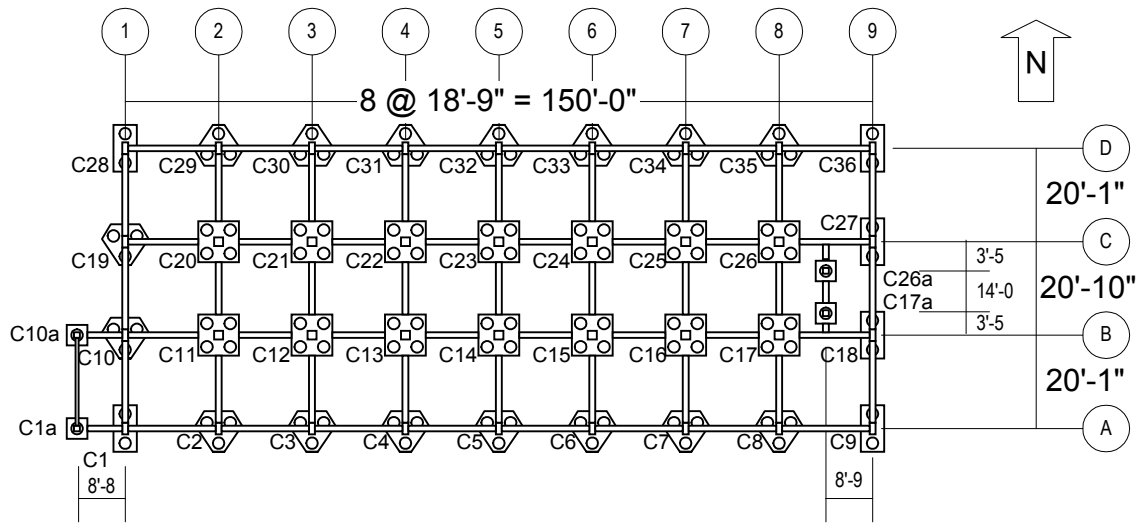


Fig. 4. Column plan.

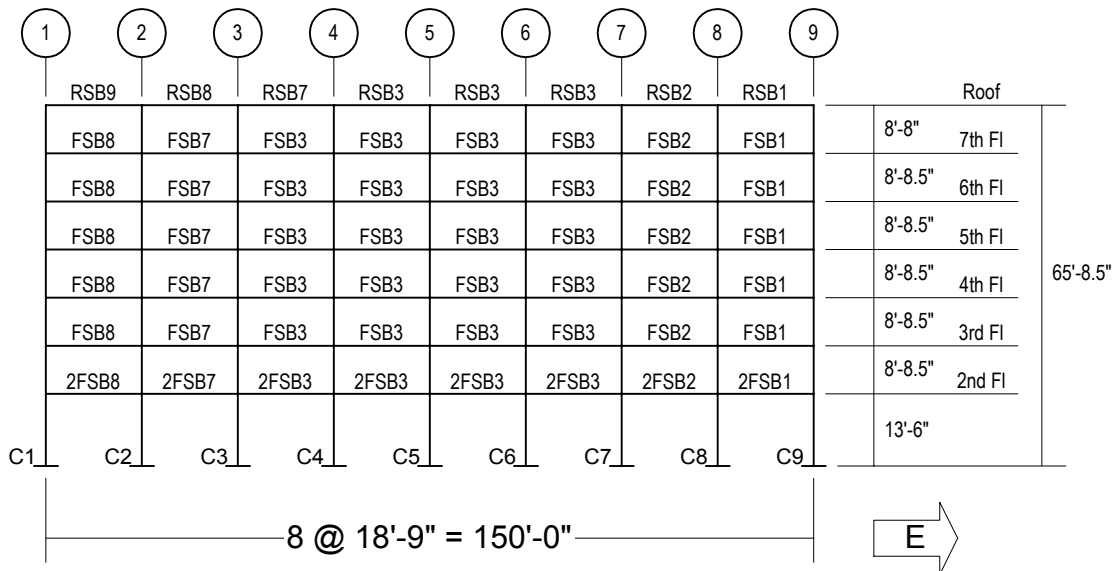


Fig. 5. South frame elevation (omitting stair tower at west end).

Floor slabs are flat plates, 10 in. thick at the 2nd floor, 8½ in. at the 3rd through 7th floors, and 8 in. at the roof. The roof also has lightweight concrete topping of varying thickness (3-1/4 in. to 8 in.). The tops of the spandrel beams are flush with the top of the floor slab.

Column concrete has nominal strength of $f'_c = 5$ ksi for the first story, 4 ksi for the second story, and 3 ksi from the third story to the seventh. Beam and slab concrete is nominally $f'_c = 4$ ksi at the second floor and 3 ksi from the third floor to the roof. Column reinforcement steel is scheduled as A432-62T (Grade 60) for billet bars. Beam and slab reinforcement is scheduled as ASTM A15-62T and A305-56T (Grade 40) for intermediate grade, deformed billet bars.

The ground floor, as it existed prior to the 1994 Northridge earthquake, contains a lobby, dining room, tavern, banquet room, and various hotel support services. Upper floors are arranged with 22 hotel suites accessed via a central corridor running the longitudinal axis of the building. The building is clad on the north and south facades with aluminum window wall, comprising 3/16-in. heavy sheet glass in sliding frames, and 1/4-in. cement asbestos board panels with an ornamental sight-obscuring mesh of baked enamel or colored vinyl. Interior partitions are constructed of 5/8-in. gypsum wallboard on 3-5/8 in. metal studs at 16-in. centers. Ceilings in the hotel suites in the 2nd through 7th stories are a textured coating applied to the soffit of the concrete slab above; at the first floor and in the upper-story hallways, ceilings are suspended wallboard or lath and plaster. The east and west endwalls are finished on the inside with gypsum wallboard and on the outside with stucco. (Examination of the structural drawings and a site inspection confirm that these are not reinforced-concrete shearwalls, as they may appear at first glance.)

Through-wall air-conditioning units are mounted in the waist panels below the windows and provide ventilation to the suites. Central heating, ventilation, and air conditioning (HVAC) is provided only for hallway and ground-floor spaces. Central HVAC equipment—fans, cooling towers, and packaged AC units—are located on the roof.

4.2 Site Hazard and Ground-Motion Selection

Soil conditions at the site are found in Tinsley and Fumal [1985], who map surficial soil deposits in the Los Angeles region using a variety of sources. They describe the site soil as Holocene fine-grained sediment (silt and clay) with a mean shear-wave velocity of 200 m/sec (and a standard deviation of 20 m/sec), corresponding to site class D, stiff soil, as defined by the International Code Council [2000], and soil profile type S_D according to the Structural Engineers Association of California [1999]. California Geosystems [1994] performed four soil borings at the site, and report that site soils are “mostly brown silty fine sand and sandy silts with some clay binder. The composition of soils is fairly consistent.” While soil densification during an earthquake is possible, the geotechnical engineers do not find liquefaction, lateral spreading, or other ground failures to be significant perils. In his study of the same building, Islam [1996b] reaches the conclusion that the “site coefficient factor [is] S2 or greater.”

The hazard for the latitude and longitude of the site is drawn from Frankel and Leyendecker [2001], who provide mean annual exceedance frequency versus S_a for periods of 1 sec and 2 sec. Their hazard curves assume soil at the boundary of classes B and C. Linearly interpolating between the two hazard curves for $T = 1.5$ sec, and adjusting for the site soil conditions (class D) using the site coefficient F_V from the International Code Council [2000], one obtains the mean site hazard shown in Fig. 6. The figure gives the mean annual exceedance frequency of damped elastic spectral acceleration S_a at the site, based on soil type D and 1.5 sec period.

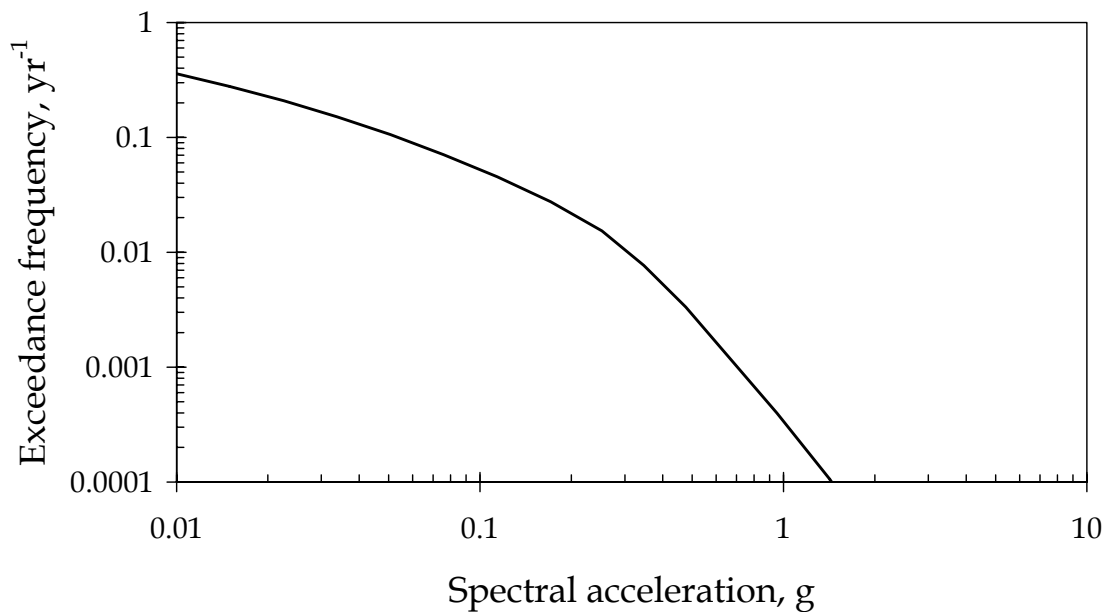


Fig. 6. Site hazard.

We select as the lower-bound, median, and upper-bound shaking intensity the S_a with nonexceedance probabilities of $P_0 = 10\%$, 50% , and 90% in $t = 50$ years, respectively. The first S_a represents an earthquake that the building is highly likely to experience in the next 50 years (10% chance of nonexceedance = 90% chance of exceedance). The last two represent events that might typically be used to test immediate-occupancy and life-safety performance objectives, respectively, for new design. Applying Equation 4 leads to the lower-bound, median, and upper-bound shaking intensities of $S_a = 0.11$, 0.27 , and $0.58g$. In fact, this building has already seen more than its fair share of earthquakes: the 1971 and 1994 earthquakes both shook it more strongly than the median event examined here.

Given the desired levels of S_a , we next select scaled ground motions to represent the 10th, 50th, and 90th percentile ground-motion time histories. To make this selection, 20 ground motions are selected at random from set of 100 available records [Somerville *et al.*, 1997]. The selection is made so that each record need be scaled in amplitude no more than $\pm 50\%$ to have $S_a = 0.27g$ (50% in 50 yr shaking). An ABV loss analysis is then performed with each scaled record, using the best-estimate values of structural characteristics, assembly capacity, unit costs, and overhead and profit.

Each analysis produces an (S_a, DF) pair. Table 3 shows the ground-motion records used, their S_a as they appear in Somerville *et al.* [1997], and an amplitude scaling factor required to produce $S_a = 0.27g$. The table shows the calculated damage factor at $S_a = 0.27g$, and the rank of the simulation by DF . We find that the correlation coefficients $\rho_{M,DF} = 0.4$ and $\rho_{R,DF} = 0.4$, both of which are less than the 5% point for the equal-tails test of the hypothesis $\rho = 0$, so one cannot reject the hypotheses that no linear relationship exists between either M and DF or R and DF , satisfying the sufficiency test proposed by Luco and Cornell [2001] for this level of S_a .

Table 3. Recordings considered for representing lower-bound, median, and upper-bound ground-motion time histories.

Record	M	R (km)	S_a , g	Scaling	DF	DF rank	Percentile
LA51	6.1	3.7	0.44	0.61	0.45	1	90 th
LA49	6.2	15	0.34	0.79	0.36	2	
LA59	6.0	17	0.19	1.41	0.35	3	
LA47	7.3	64	0.32	0.85	0.30	4	
LA01	6.9	10	0.19	1.44	0.29	5	
NF02	7.4	1.2	0.17	1.61	0.28	6	
LA55	6.0	9.6	0.32	0.85	0.26	7	50 th
LA56	6.0	9.6	0.40	0.68	0.26	8	
LA02	6.9	10	0.20	1.36	0.26	9	
LA19	6.0	6.7	0.25	1.08	0.24	10	
LA54	6.1	8.0	0.34	0.79	0.23	11	
LA17	6.7	6.4	0.16	1.73	0.23	12	
NF08	7.1	8.5	0.15	1.77	0.22	13	
LA08	7.3	36	0.21	1.28	0.22	14	
LA07	7.3	36	0.23	1.20	0.21	15	
LA50	6.2	15	0.34	0.78	0.21	16	
LA53	6.1	8.0	0.42	0.65	0.20	17	10 th
LA46	7.7	107	0.38	0.71	0.16	18	
LA45	7.7	107	0.30	0.91	0.14	19	
LA58	6.5	1.0	0.27	1.00	0.14	20	

Of the 20 records examined, LA45 produces the 10th-percentile DF , LA19 and LA54 produce the median values, and LA49, the 90th percentile. Either LA19 or LA54 should be taken as the median, but in the analyses presented here, LA50 was erroneously used. Its damage factor is close to the median, so the associated error is likely modest.

4.3 Structural Model

The building weighs approximately 134 psf, based on structural and architectural quantities and unit weights. This is mostly attributable to the 8½-in normal-weight concrete slabs (106 psf), and the columns and spandrel beams (18 psf of deck). The balance (10 psf) is added to account for architectural finishes, and mechanical, electrical, and plumbing components. Bounding values for mass are based on a Gaussian distribution with a coefficient of variation of 0.10. All masses are increased or decreased by the appropriate amount (i.e., masses are taken as perfectly correlated). Rayleigh damping is taken as 5% of critical with Gaussian distribution and coefficient of variation taken to be 0.40.

The design information is used to create a model for structural analysis. The south frame, which was heavily damaged in the 1994 Northridge earthquake, is selected for modeling in a 2-D nonlinear time-history structural analysis. Material nonlinearities are considered, and geometric nonlinearities ignored. The moment-curvature and P-M interaction characteristics of the reinforced-concrete members are assessed using UCFyber [ZEvent, 2000]. The cylinder strength of reinforced concrete is taken as the 28-day nominal value, plus 1.5 standard deviations ($\sigma = 600$ psi for $f'_c \geq 4$ ksi) to account for initial overstrength, plus an additional 69% to account for concrete age (+30%) and earthquake strain rate (+30%).

The flexural behavior of the beams and columns is represented by a one-component Giberson beam with plastic hinges at the ends [Sharpe, 1974]. The shear deformation for the beams is assumed to be elastic and is incorporated in the flexural elements. The shear deformation for the columns is modeled by inelastic springs attached to the ends of the flexural elements. Centerline dimensions are used with rigid-block offsets to account for joint stiffness.

Two hysteresis rules are used to model reinforced-concrete members' nonlinear behavior: the SINA tri-linear hysteresis rule [Saiidi and Sozen, 1979] is used to model stiffness

degradation of reinforced-concrete members in flexure. The Q-HYST bi-linear hysteresis [Saiidi and Sozen, 1979] is used to model the stiffness degradation of reinforced-concrete members in shear. Strength degradation using Pincheira *et al.* [1999] is applied to both hysteretic rules. The structural analyses are performed using Ruaumoko [Carr, 2001].

4.4 Assembly Capacity and Repair Costs

Assembly fragility functions and repair costs have been developed for all of the damageable assemblies in the building (see Porter and Kiremidjian [2001b], Beck *et al.* [1999], and Beck *et al.* [2002]), using laboratory test data for reinforced-concrete beam-columns, drywall, and stucco partitions. Window fragility is based on theoretical considerations for window glazing by comparing theoretical glass strain as a function of drift angle with observed glass fracture strain.

As the application of these fragility functions may be unfamiliar to the reader, it is worthwhile to summarize their use in an ABV analysis. For each assembly, let N_D denote the number of possible damage states other than undamaged. Let each damage state be denoted by an integer that increases with increasing severity of damage. Thus, each assembly must be in one damage state $d \in \{0, 1, \dots, N_D\}$, where $d = 0$ denotes a state of no damage. For a lognormal fragility function, the probability that a particular assembly will reach or exceed a particular damage state d , conditioned on the structural response z to which it is subjected, is

$$P_z(d) = P[D \geq d \mid Z = z] = \Phi\left(\frac{\ln(z/x_m(d))}{\beta(d)}\right) \quad (7)$$

where D is the uncertain damage state of a particular assembly, d is a possible damage state of that assembly, Z is the uncertain structural response to which the assembly is subjected, z is the calculated response from a particular simulation, and x_m and β are parameters of the fragility function, defined for each assembly type and damage state d .

In a probabilistic loss analysis, damage is simulated for each assembly and each simulation as follows. The structural analysis produces the structural response z to which the assembly is subjected. Equation 7 is evaluated for each possible damage state. A random sample u is drawn from a uniform probability distribution over $[0, 1]$; this value is compared

with each failure probability $P_z(d)$ for $d = 1, 2, \dots, N_D$. The assembly is said to have reached or exceeded damage state d if $u \leq P_z(d)$. The maximum damage state d_m reached or exceeded is the final simulated damage state of the assembly. That is,

$$d_m = \max d : u \leq P_z(d) \quad (8)$$

Note that the probability that an assembly is in damage state d , denoted by $P[D=d|Z=z]$, is equal to $1 - P_z(1)$ for $d = 0$ (the undamaged state), or $P_z(d) - P_z(d+1)$ for $1 \leq d < N_D$, or $P_z(d)$ for $d = N_D$ (the most severe damage state).

Fragility functions for assemblies in the demonstration building, derived in Beck *et al.* (2002), are summarized in Table 4. Repair costs, provided by a professional cost estimator, are summarized in Table 5. In this table, the parameters x_m and β represent the median and logarithmic standard deviation of the cost to restore one unit of the assembly from damage state d to the undamaged state. The table shows the nature of the repair. The units by which the assemblies are measured are shown in the column labeled "Unit." Unit costs are in dollars in 2001. For derivation details, see Beck *et al.* [2002].

Contractor overhead and profit is taken as uniformly distributed between 0.15 and 0.20 times the total direct cost. Thus, the total repair cost is given by

$$C_R = (1 + C_{O\&P}) \left(\sum_{j=1}^{N_J} \sum_{d=1}^{N_{D,j}} C_{j,d} N_{j,d} \right) \quad (9)$$

but economic performance is more often expressed in terms of a damage factor (defined as the ratio of repair cost to replacement cost):

$$DF = C_R / RCN \quad (10)$$

where

C_R = cost to repair the building

$C_{O\&P}$ = contractor overhead-and-profit factor, assumed to be uniformly distributed between 0.15 and 0.20, per the cost estimator.

$C_{j,d}$ = cost to restore one unit of assembly type j from damage state d

DF = damage factor

$N_{D,j}$ = number of possible damage states for assembly type j

N_J = number of damageable assembly types present in the building

$N_{j,d}$ = number of assemblies of type j in damage state d

RCN = replacement cost (new)

To study the effect of uncertain capacity on overall loss uncertainty, we take all the capacity values at their 10th, 50th, and 90th percentiles, to represent lower-bound, best-estimate, and upper-bound assembly capacity, respectively. This is as opposed to allowing capacity to vary randomly in each assembly (per the normal, probabilistic ABV approach) or varying the capacity of each assembly type sequentially, e.g., varying only the capacity of reinforced-concrete beam-columns, then only that of wallboard partitions, etc. The latter approach would be more informative of the effect of each individual assembly type, but would tend to emphasize the details rather than the general importance of assembly damageability.

Table 4. Summary of assembly fragility parameters.

Assembly type	Description	d	Limit State	Resp	x_m	β
6.1.510.1202.02	Stucco finish, 7/8", on 3-5/8" mtl stud, 16"OC	1	Cracking	PTD	0.012	0.5
6.1.500.0002.01	Drywall finish, 5/8-in., 1 side, on metal stud, screws	1	Visible dmg	PTD	0.0039	0.17
6.1.500.0002.01	Drywall finish, 5/8-in., 1 side, on metal stud, screws	2	Signif. dmg	PTD	0.0085	0.23
6.1.500.0001.01	Drywall partition, 5/8-in., 1 side, on metal stud, screws	1	Visible dmg	PTD	0.0039	0.17
6.1.500.0001.01	Drywall partition, 5/8-in., 1 side, on metal stud, screws	2	Signif. dmg	PTD	0.0085	0.23
3.5.180.1101.01	Nonductile CIP RC column	1	Light	PADI	0.080	1.36
3.5.180.1101.01	Nonductile CIP RC column	2	Moderate	PADI	0.31	0.89
3.5.180.1101.01	Nonductile CIP RC column	3	Severe	PADI	0.71	0.8
3.5.180.1101.01	Nonductile CIP RC column	4	Collapse	PADI	1.28	0.74
3.5.190.1102.01	Nonductile CIP RC beam	1	Light	PADI	0.080	1.36
3.5.190.1102.01	Nonductile CIP RC beam	2	Moderate	PADI	0.32	0.89
3.5.190.1102.01	Nonductile CIP RC beam	3	Severe	PADI	0.71	0.8
3.5.190.1102.01	Nonductile CIP RC beam	4	Collapse	PADI	1.28	0.74
4.7.110.6700.02	Window, Al frm, sliding, hvy sheet glass, 4'x2'-6"x3/16"	1	Cracking	PTD	0.023	0.28

Resp = type of structural response used as excitation in the fragility function

PTD = peak transient drift ratio

PADI = Modified Park-Ang damage index (displacement portion): $(\phi_m - \phi_y)/(\phi_u - \phi_y)$, where ϕ_m = maximum curvature, ϕ_y = yield curvature, ϕ_u = curvature at maximum moment for the element in question, considering the element's own material and geometric properties

x_m = median capacity; β = logarithmic standard deviation of capacity

Table 5. Summary of unit repair costs.

Assembly Type	Description	d	Repair	Unit	x_m	β
6.1.510.1202.02	Stucco finish, 7/8", on 3-5/8" mtl stud, 16"OC	1	Patch	64 sf	125	0.2
6.1.500.0002.01	Drywall finish, 5/8-in., 1 side, on metal stud, screws	1	Patch	64 sf	88	0.2
6.1.500.0002.01	Drywall finish, 5/8-in., 1 side, on metal stud, screws	2	Replace	64 sf	253	0.2
6.1.500.0001.01	Drywall partition, 5/8-in., 1 side, on metal stud, screws	1	Patch	64 sf	88	0.2
6.1.500.0001.01	Drywall partition, 5/8-in., 1 side, on metal stud, screws	2	Replace	64 sf	525	0.2
3.5.180.1101.01	Nonductile CIP R/C column	1	Epoxy	ea	8000	0.42
3.5.180.1101.01	Nonductile CIP R/C column	2	Jacket	ea	20500	0.4
3.5.180.1101.01	Nonductile CIP R/C column	3,4	Replace	ea	34300	0.37
3.5.190.1102.01	Nonductile CIP R/C beam	1	Epoxy	ea	8000	0.42
3.5.190.1102.01	Nonductile CIP R/C beam	2	Jacket	ea	20500	0.4
3.5.190.1102.01	Nonductile CIP R/C beam	3,4	Replace	ea	34300	0.37
4.7.110.6700.02	Window, Al frame, sliding, hvy sheet glass, 4'-0x2'-6"x3/16"	1	Replace	ea	180	0.2
09910.700.1400	Paint on exterior stucco or concrete	1	Paint	sf	1.45	0.2
09910.920.0840	Paint on interior concrete, drywall, or plaster	1	Paint	sf	1.52	0.2

Likewise, to study the effect of uncertainty in contractor costs, we take all the unit-cost values at their 10th, 50th, and 90th percentiles simultaneously to represent lower-bound, best-estimate, and upper-bound of direct costs to the contractor. We employ mean values and uncertainties in unit costs provided by professional cost estimators [Young, 2001, and Machin, 2001]. In cases where the estimator judged the coefficient of variation for unit costs to be less than 0.20, we applied 0.20 as a minimum value, in light of RS Means Corp.'s [1997] cost contingency for repair. It would be highly desirable to collect empirical data on unit-cost uncertainty, in order to avoid this conscious and somewhat arbitrary application of judgment.

Finally, we take the lower bound (0.15), median, and upper-bound (0.20) values of $C_{O\&P}$ to determine the effect of uncertainty in the overhead and profit costs charged by the contractor.

5. Study Results

Table 6 summarizes the input parameters used in the sensitivity study. Results of the sensitivity study are shown in Table 7, and depicted graphically in the tornado diagram of Fig. 7. The table shows the damage factor (repair cost divided by replacement cost) that results when all parameters are set to their best-estimate value, except for one parameter, set to its low or high value. The ends of each bar in the tornado diagram indicate the outcome using the low and high values of that parameter. The length of the bar indicates the absolute difference (“swing”) between the damage factors from the low and high values of the changed parameter, i.e., the deterministic sensitivity of the damage factor to that parameter.

The baseline damage factor (i.e., the damage factor that was calculated using best-estimate values of all parameters) is $DF = 0.21$, at $S_a = 0.27g$. This is approximately equal to the shaking intensity experienced by the building during the 1971 San Fernando earthquake (0.34g), which resulted in a damage factor of approximately 0.11, which is reasonably within the range of uncertainty reflected in Fig. 7.

Table 6. Parameters of the sensitivity study.

Parameter	Lower bound	Best estimate	Upper bound	Comment
S_a (g)	0.11 (LA50, 0.52)	0.27 (LA50, 1.28)	0.58 (LA50, 2.74)	Spectral acceleration (Record, scaling factor)
Ground motion	LA45, 1.10	LA50, 1.28	LA49, 1.26	Record, scaling factor
Mass	$0.872M_n$	M_n	$1.128M_n$	M_n : nominal mass
Damping	2.4%	5.0%	7.6%	Percent of critical
Force-deformation multiplier	0.90	1.00	1.10	Factor applied to F & d in F - d relationships
Assembly capacity	$e^{\ln(x_m)-1.28\beta}$	x_m	$e^{\ln(x_m)+1.28\beta}$	x_m and β from Table 4
Costs: unit cost	$e^{\ln(x_m)-1.28\beta}$	x_m	$e^{\ln(x_m)+1.28\beta}$	x_m and β from Table 5
O&P	0.15	0.175	0.20	$C_{O\&P}$ of Equation 11

Table 7. Summary of results.

Parameter X	Damage factor (DF)		
	DF (low X)	DF (high X)	Swing
Assembly capacity	0.94	0.06	0.87
S_a	0.03	0.66	0.63
Ground motion record	0.14	0.36	0.22
Unit cost	0.13	0.33	0.20
Damping	0.29	0.15	0.14
F-d multiplier	0.23	0.17	0.07
Mass	0.20	0.22	0.02
O&P	0.20	0.21	0.01

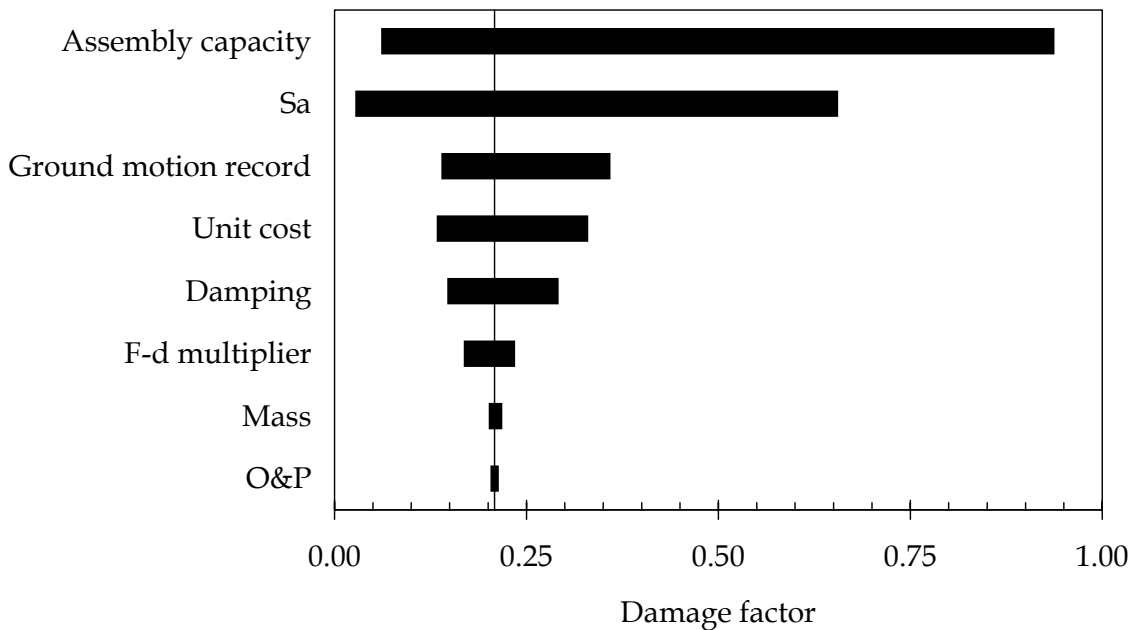


Fig. 7. Results of the sensitivity study.

Fig. 7 reflects only the 7-story nonductile reinforced-concrete building structure in Van Nuys, but it offers some intriguing implications:

1. First, the greatest part of performance uncertainty is due to the uncertainty in the capacity of building assemblies to resist damage. This may be more readily reduced with additional knowledge than is the uncertainty in the shaking intensity of future earthquakes.

2. The figure suggests that uncertainty in the features that affect structural response (mass, damping, and the hysteretic behavior of the structural elements) are relatively minor contributors to overall performance uncertainty. That is, uncertainty in the structural analysis is significantly less important than uncertainty in the damage analysis. (By *damage analysis*, we mean the portion of the performance analysis that estimates physical damage, given structural response.)
3. There is modest swing associated with the ground motion record after conditioning on S_a . This implies that S_a alone is a fairly good intensity measure at the 50%/50 yr hazard level. The swing associated with the ground-motion record is comparable with that of the contractor's unit costs. This implies that a better intensity measure than S_a could produce only a modest reduction in overall uncertainty.

Another data point is the study by Porter and Kiremidjian [2001b] of a hypothetical pre-Northridge welded-steel moment-frame building. That study neglects uncertainties in structural characteristics, but it does produce a similarly large swing associated with the capacity of building components, most notably the capacity of pre-Northridge steel moment-frame connections.

6. Conclusions

This report summarizes a deterministic sensitivity study for a highrise nonductile reinforced-concrete moment-frame building in Van Nuys, California. The study examines the sensitivity of the building's future economic performance (repair cost) to a number of basic uncertain variables, including shaking intensity, ground motion, structural characteristics, assembly damageability, and repair costs.

For this building, the overall economic performance, as measured in terms of damage factor conditioned on the (uncertain) largest S_a for the site in the next 50 years, is primarily sensitive to uncertainty in assembly capacity and shaking intensity (parameterized via spectral acceleration response at the building's small-amplitude fundamental period and 5% damping). Loss is moderately sensitive to details of the ground motion (reflected in the variability of the repair cost for the best-estimate model, subjected to 20 different ground motions of the same shaking intensity S_a), and to the contractor's unit costs. Uncertainty in structural characteristics (mass, damping, and hysteretic behavior) also have a modest effect on performance, although they individually account for less uncertainty than the contractor's unit repair costs.

While these results consider only the demonstration building, they suggest the possibility that uncertainty in performance can be best reduced via better understanding of damageability of building components. They also suggest that a deterministic (best-estimate) structural model may be adequate for performance evaluation of buildings, and that better intensity measures might not substantially reduce uncertainty in economic performance. Such suggestions should be examined by similar studies of additional buildings.

Several potentially important sources of uncertainty are not examined here, e.g., seismic hazard parameters, union vs. nonunion labor; demand surge; building-code changes that would require additional strengthening beyond mere repair; the potential for the actual future repair method to differ from that assumed here; the potential that needed repairs will not be performed;

and the possibility that preexisting damage will be imputed to the earthquake. Each of these topics is worthy of additional study.

References

- American Society for Testing and Materials (ASTM), 1996, E1557-96 Standard classification for building elements and related sitework – UNIFORMAT II, *1997 Annual Book of ASTM Standards, Section 4, Construction, Volume 04.11 Building Constructions*, West Conshohocken, PA, 630-639.
- Applied Technology Council, 1985, *ATC-13, Earthquake Damage Evaluation Data for California*, Redwood City, CA, 492 pp.
- Beck, J.L., 1982, System identification applied to strong motion records from structures, *Earthquake Ground Motion and its Effects on Structures*, S.K. Datta, ed., American Society of Mechanical Engineers, New York, 109-134.
- Beck, J.L., Kiremidjian, A., Wilkie, S., Mason, A., Salmon, T., Goltz, J., Olson, R., Workman, J., Irfanoglu, A., and Porter, K., 1999, *Decision Support Tools for Earthquake Recovery of Businesses, Final Report, CUREE-Kajima Joint Research Program Phase III*, Consortium of Universities for Earthquake Engineering Research, Richmond, CA.
- Beck, J.L., Porter, K.A., Shaikhutdinov, R., Moroi, T., Tsukada, Y., and Masuda, M., 2002 (in press), *Impact of Seismic Risk on Lifetime Property Values, Final Report, CUREE-Kajima Joint Research Program Phase IV*, Consortium of Universities for Earthquake Engineering Research, Richmond, CA.
- Browning, J., Li, Y., Lynn, A., and Moehle, J.P., 2000, Performance assessment for a reinforced concrete frame building, *Earthquake Spectra*, **16** (3), Earthquake Engineering Research Institute, Oakland, CA, 541-555.
- California Geosystems, 1994, *Foundation Soils Investigation, Existing Holiday Inn Building, Roscoe Blvd and Orion Ave, Van Nuys, CA*, Glendale, CA, 26 pp.
- Camelo, V.S., Beck, J.L., and Hall, J.F., 2001, *Dynamic Characteristics of Woodframe Structures*, Richmond, CA: Consortium of Universities for Research in Earthquake Engineering, 68 pp.
- Carr, A.J., 2001, *Ruaumoko 2-D*, University of Canterbury, Christchurch, New Zealand.
- Cordova, P.P., Deierlein, G.G., Mehanny, S.S.F., and Cornell, C.A., 2001, Development of a two-parameter seismic intensity measure and probabilistic assessment procedure, *2nd U.S.-Japan Workshop on Performance-Based Earthquake Engineering for Reinforced Concrete Building Structures 11–13 September 2000 in Sapporo, Japan*, Pacific Earthquake Engineering Research Center, Richmond, CA.
- Ellingwood, B., Galambos, T.V., MacGregor, J.G., and Cornell, C.A., 1980, *Development of a Probability-Based Load Criterion for American National Standard A58*, National Bureau of Standards, Washington, DC, 222 pp.
- Federal Emergency Management Agency, 1997, *FEMA-273: NEHRP Guidelines for the Seismic Rehabilitation of Buildings*, Washington, DC, 386 pp.
- Federal Emergency Management Agency, 2000, *FEMA-356: Prestandard and Commentary for the Seismic Rehabilitation of Buildings*, Washington, DC.
- Frankel, A., and Leyendecker, E.V., 2001, *Uniform Hazard Response Spectra and Seismic Hazard Curves for the United States*, US Geological Survey, Menlo Park, CA.

- Hart, G.C., and Vasdevan, R., 1975, Earthquake Design of Buildings: Damping, *Journal of the Structural Division*, 101 (ST1), Jan 1975, American Society of Civil Engineers, 11-29.
- International Code Council, 2000, *International Building Code 2000*, International Conference of Building Officials, Whittier, CA, 756 pp.
- Islam, M.S., 1996a, Analysis of the response of an instrumented 7-story nonductile concrete frame building damaged during the Northridge Earthquake, *Proceedings of the 1996 Annual Meeting of the Los Angeles Tall Buildings Structural Council, May 10, 1996, Los Angeles, CA*.
- Islam, M.S., 1996b, Holiday Inn, 1994 Northridge Earthquake Buildings Case Study Project Proposition 122: Product 3.2, Seismic Safety Commission, Sacramento CA, 189-233.
- Islam, M.S., Gupta, M., and Kunnath, B., 1998, Critical review of the state-of-the-art analytical tools and acceptance criterion in light of observed response of an instrumented nonductile concrete frame building, *Proceedings, Sixth US National Conference on Earthquake Engineering, Seattle, Washington, May 31-June 4, 1998*, Earthquake Engineering Research Institute, Oakland CA, 11 pp.
- Jennings, P.C., 1971, *Engineering Features of the San Fernando Earthquake of February 9, 1971, Report EERL 71 - 02*, California Institute of Technology, Pasadena, CA.
- Li, Y.R., and Jirsa, J.O., 1998, Nonlinear analyses of an instrumented structure damaged in the 1994 Northridge Earthquake, *Earthquake Spectra*, **14** (2), Earthquake Engineering Research Institute, Oakland, CA, 245-264.
- Luco, N., and Cornell, C.A., in press, Structure-specific scalar intensity measures for near-source and ordinary earthquake ground motions, Submitted for publication, April, 2001, *Earthquake Spectra*, http://pitch.stanford.edu/rmsweb/RMS_Papers/pdf/nico/EQ_Spectra01.pdf.
- Machin, J., 2001, personal communication.
- McVerry, G.H., 1979, *Frequency Domain Identification of Structural Models for Earthquake Records, Report No. EERL 79-02*, California Institute of Technology, Pasadena, CA, <http://caltecheerl.library.caltech.edu/documents/disk0/00/00/02/23/00000223-00/7902.pdf>, 221 pp.
- Pincheira, J.A., Dotiwala, F.S., and D'Souza, J.T., 1999, Seismic analysis of older reinforced concrete columns, *Earthquake Spectra*, **15** (2), Earthquake Engineering Research Institute, Oakland, CA, 245-272.
- Porter, K.A., and Kiremidjian, A.S., 2001b, *Assembly-based Vulnerability and its Uses in Seismic Performance Evaluation and Risk-Management Decision-Making*, John A. Blume Earthquake Engineering Center, Stanford, CA, 214 pp.
- Porter, K.A., Beck, J.L., Seligson, H.A., Scawthorn, C.R., Tobin, L.T., Young, R., and Boyd, T., 2001c, *Improving Loss Estimation for Woodframe Buildings, Draft Final Report, Vol. 2*, Consortium of Universities for Research in Earthquake Engineering, Richmond, CA, http://www.curee.org/projects/woodframe_project/element4/task_4_1.html.
- Porter, K.A., Kiremidjian, A.S., and LeGrue, J.S., 2001a, Assembly-based vulnerability of buildings and its use in performance evaluation, *Earthquake Spectra*, **17** (2), Earthquake Engineering Research Institute, Oakland, CA, 291-312.
- Rissman and Rissman Associates, 1965, *Holiday Inn Van Nuys Structural Drawings*, Pacific Palisades, CA.
- RS Means Co., Inc., 1997, *Means Assemblies Cost Data*, Kingston, MA.
- Saiidi, M., and Sozen, M.A., 1979, *Simple and Complex Models for Nonlinear Seismic Response of Reinforced Concrete Structures, Report UILU-ENG-79-2031*, Department of Civil Engineering, University of Illinois, Urbana, IL.
- Scholl, R.E., Kustu, O., Perry, C.L., and Zanetti, J.M., 1982, *Seismic Damage Assessment for High-Rise Buildings, URS/JAB 8020*, URS/John A. Blume & Associates, Engineers, San Francisco, CA, 321 pp.

- Sharpe, R.D., 1974, *The Nonlinear Response of Inelastic Structures*, Ph.D. Thesis, Department of Civil Engineering, University of Canterbury, Christchurch, New Zealand.
- Somerville, P., Smith, N., Punyamurthula, S., and Sun, S., 1997, *Development of Ground Motion Time Histories for Phase 2 of the FEMA/SAC Steel Project*, SAC Joint Venture, Background Document Report No. SAC/BD-97/04.
- Structural Engineers Association of California, 1999, *Recommended Lateral Force Requirements and Commentary*, 7th Edition, Sacramento, CA, 440 pp.
- Taoko, G.T., 1981, Damping measurements of tall structures, *Proc. Second Specialty Conference on Dynamic Response of Structures: Experimentation, Observation, Prediction, and Control*, January 15-16, 1981, Atlanta, GA, American Society of Civil Engineers, New York, NY, 308-322.
- Tinsley, J.C., and Fumal, T.E., 1985, Mapping Quaternary sedimentary deposits for areal variations in shaking response, *Evaluating Earthquake Hazards in the Los Angeles Region—An Earth-Science Perspective*, U.S. Geological Survey Professional Paper 1360, U.S. Government Printing Office, Washington DC, 101-126.
- Young, R., 2001, personal communication.
- ZEvent, 2000, *UCFyber Version 2.4.1*, Berkeley, CA.